Immune Netw. 2023 Oct;23(5):e42
https://doi.org/10.4110/in.2023.23.e42
pISSN 1598-2629·eISSN 2092-6685

IMMUNE NETWORK

Original Article

NADPH Oxidase 4-mediated Alveolar Macrophage Recruitment to Lung Attenuates Neutrophilic Inflammation in *Staphylococcus aureus* Infection

Seunghan Han, Sungmin Moon, Youn Wook Chung, Ji-Hwan Ryu *

Department of Biomedical Sciences, Graduate School of Medical Science, Brain Korea 21 Project, Yonsei University College of Medicine, Seoul 03722, Korea

Received: Apr 14, 2023
Revised: Sep 25, 2023
Accepted: Oct 22, 2023
Published online: Oct 27, 2023

***Correspondence to**
Ji-Hwan Ryu
Department of Biomedical Sciences, Graduate School of Medical Science, Brain Korea 21 Project, Yonsei University College of Medicine, 50-1 Yonsei-ro, Seodaemun-gu, Seoul 03722, Korea.
Email: yjh@yuhs.ac

ORCID iDs
Seunghan Han
https://orcid.org/0000-0003-3627-8015
Sungmin Moon
https://orcid.org/0000-0002-1142-2079
Youn Wook Chung
https://orcid.org/0000-0002-4382-1410
Ji-Hwan Ryu
https://orcid.org/0000-0001-6969-7465

Conflict of Interest
The authors declare no potential conflicts of interest.

ABSTRACT

When the lungs are infected with bacteria, alveolar macrophages (AMs) are recruited to the site and play a crucial role in protecting the host by reducing excessive lung inflammation. However, the regulatory mechanisms that trigger the recruitment of AMs to lung alveoli during an infection are still not fully understood. In this study, we identified a critical role for NADPH oxidase 4 (NOX4) in the recruitment of AMs during *Staphylococcus aureus* lung infection. We found that NOX4 knockout (KO) mice showed decreased recruitment of AMs and increased lung neutrophils and injury in response to *S. aureus* infection compared to wild-type (WT) mice. Interestingly, the burden of *S. aureus* in the lungs was not different between NOX4 KO and WT mice. Furthermore, we observed that depletion of AMs in WT mice during *S. aureus* infection increased the number of neutrophils and lung injury to a similar level as that observed in NOX4 KO mice. Additionally, we found that expression of intercellular adhesion molecule-1 (ICAM1) in NOX4 KO mice-derived lung endothelial cells was lower than that in WT mice-derived endothelial cells. Therefore, we conclude that NOX4 plays a crucial role in inducing the recruitment of AMs by controlling ICAM1 expression in lung endothelial cells, which is responsible for resolving lung inflammation during acute *S. aureus* infection.

Keywords: Alveolar macrophage; *Staphylococcus aureus*; NADPH oxidase 4; Bacterial infections

INTRODUCTION

Alveolar macrophages (AMs) are the predominant immune cells in the lungs and play a key role in maintaining lung homeostasis (1-3). During severe situations, such as bacterial infections, monocytes are recruited from the bloodstream to the alveoli (4). For recruitment of the monocytes, LFA1 and MAC1 on the monocytes bind to endothelial intercellular adhesion molecule-1 (ICAM1), and then the monocytes proceed to rolling, crawling, and transmigration (5,6). The recruited monocytes then differentiate into monocyte-derived AMs (7). The AMs reduce excessive inflammation and effect resolution of inflammation by producing anti-inflammatory and repair factors (8-10). However, the regulatory role of AM recruitment into the alveoli in bacterial infection is not well defined.

IMMUNE NETWORK

Abbreviations

AM, alveolar macrophage; BALF, bronchoalveolar lavage fluid; BHI, Brain Heart Infusion; BMDN, bone-marrow derived neutrophils; CAP, community-acquired pneumonia; CFU, colony forming unit; ICAM1, intercellular adhesion molecule-1; KO, knockout; MACS, magnetic-activated cell sorting; MFI, mean fluorescence intensity; MOI, multiplicity of infection; n.s., not significant; NOX, NADPH oxidase; PI, propidium iodide; rhVEGF165, recombinant human VEGF 165; RT, room temperature; TTBS, Tris-buffered saline with Tween 20; VEGFR2, VEGF receptor 2; WT, wild-type

Author Contributions

Conceptualization: Ryu JH; Data curation: Han S, Ryu JH; Formal analysis: Han S, Ryu JH; Funding acquisition: Ryu JH; Investigation: Moon S; Project administration: Han S, Chung YW, Ryu JH; Supervision: Ryu JH; Writing - review & editing: Ryu JH.

Bacterial pneumonia is associated with high rates of morbidity and mortality, particularly in individuals with compromised immune systems or those who are hospitalized (11,12). In patients with immune-compromise or community-acquired pneumonia (CAP), *Staphylococcus aureus* has been identified as a cause of lung infection (13,14). *S. aureus* is a gram-positive bacterium and a commensal microbe in the upper respiratory tract and on the skin (15). Although *S. aureus* is known as a respiratory pathogen and a nosocomial pathogen, research on its virulence mechanisms has focused primarily on microbial factors (16). Moreover, host defense mechanisms against *S. aureus* have been predominantly studied in relation to neutrophils (17). Therefore, identifying the regulatory mechanisms of immune cells other than neutrophils against *S. aureus* infection is necessary.

NADPH oxidases (NOX), such as NOX2, NOX4, and DUOX, are known to be host proteins that produce ROS in several cell types in the lung (18). NOX4 is a major source of cellular superoxide anion, which is involved in the biological functions of cell survival, differentiation, and apoptosis (19-21). NOX4 increases ICAM1 expression in the endothelium via the interaction of TLR5 with flagellin (22). NOX4 in inflammatory macrophages enhances NLRP3 inflammasome activation via fatty acid oxidation against *Streptococcus pneumoniae* (23). And NOX4 in macrophages helps to block *Toxoplasma gondii* infection (24). Moreover, knockdown of NOX4 in lung attenuates pulmonary permeability after *Pseudomonas aeruginosa* infection (25). According to these studies, NOX4 plays a variety of roles against various pathogens. However, the specific immunologic role of NOX4 in response to *S. aureus* lung infection remains unclear.

Here, we demonstrated that VEGF induces ICAM1 expression in a NOX4-dependent manner, resulting in the recruitment of AMs into the lung. Additionally, we showed that AM recruitment is crucial for resolving neutrophilic inflammation in mice with NOX4 following *S. aureus* infection. These findings shed new light on the protective role of NOX4, highlighting the connection between VEGF and AM recruitment against *S. aureus* infection.

MATERIALS AND METHODS

Animals

Male C57BL/6 mice were purchased from Orient Bio (Seongnam, Korea). NOX4 knockout (KO) mice on a C57BL/6 background were bred at the animal facility of Yonsei University. Age-matched, 8- to 12-wk-old mice were used for all experiments. Mice were housed under specific pathogen-free conditions and maintained in a 12 h light-dark cycle until the start of each experiment. All experiments were performed in accordance with the guidelines of the Association for Assessment and Accreditation of Laboratory Animal Care International (AAALAC International) and were approved by the Institutional Animal Care and Use Committee (IACUC) of Yonsei University Health System.

Preparation of *S. aureus*

S. aureus (ATCC 29213) was grown on a Brain Heart Infusion (BHI) agar plate at 37°C overnight. The *S. aureus* colonies were inoculated into 10 ml of fresh BHI medium and cultured in a shaking incubator at 37°C overnight. The cultured *S. aureus* was inoculated into fresh BHI medium and grown in the shaking incubator until it reached OD600 values of 1. GFP-tagged *S. aureus* was cultured on a BHI agar plate with tetracycline (100 μg/ml) at 37°C overnight. GFP-tagged *S. aureus* was grown in BHI medium containing tetracycline (100 μg/ml) until OD600 values of 1.

https://doi.org/10.4110/in.2023.23.e42

Bacterial infection model

Mice were anesthetized by zoletil/rompun mixture. The mice were intranasally instilled with 3×10^7 colony forming units (CFUs) of *S. aureus* in 40 μl PBS. Control mice were intranasally instilled with 40 μl PBS. After the infection, mice were sacrificed at the indicated time points (0, 12, 24, 48, 72, and 120 h).

Bronchoalveolar lavage fluid (BALF) and lung tissue sample collection

Mice were sacrificed by administering an overdose of the zoletil/rompun mixture. BALF was obtained by injecting 1 ml of ice-cold PBS into the trachea using a catheter. The aspiration was repeated twice until no further fluid was collected. The collected BALF was centrifuged at 4,000 rpm for 5 min at 4°C. The supernatant was used for cytokine measurement, while the pellet was counted using a hemocytometer and stained for flow cytometry. Through the right ventricle, 10 ml of ice-cold PBS were perfused into the lungs. The left lobe of the lung was fixed with 4% paraformaldehyde for H&E staining, while the right lobes of the lung were extracted and chopped into small pieces. The right lobes of the lung were dissociated with collagenase type II solution (0.005 g collagenase type II and 1 μl DNase in 5 ml PBS per mouse) for 1 h at 37°C. After dissociation, the samples were filtered twice through a 70 μm strainer and then centrifuged at 4,000 rpm for 5 min. The pellet was stained and then isolated using FACS or magnetic-activated cell sorting (MACS).

Histological inflammatory score

H&E staining of the lung section was examined and assessed through BX53 microscope (Olympus Corporation, Tokyo, Japan). The section was analyzed and qualified through random selection. Using a score, the degree of lung inflammation was assessed. Briefly, a score of 0 meant there were no leukocytes around bronchioles or alveoli; a score of 1 meant there were a few leukocytes there; a score of 2 meant there were 1–3 layers of leukocytes there; and a score of 3 meant there were 5 layers of leukocytes there.

Immunofluorescence stain

The paraffin-embedded lung tissue was stained to identify neutrophils and macrophages. After deparaffinization and rehydration using xylene at decreasing concentrations (100% to 50%), the slides underwent heat-induced Ag retrieval in 10 mM sodium citrate buffer (pH 6.0) for 20 min at 95°C. The slides were then blocked with PBS containing 2% BSA and 2% donkey serum for 2 h at room temperature (RT). They were stained with DAKO Ab diluent (Agilent, Carpinteria, CA, USA), including neutrophil Abs (Abcam, Cambridge, UK) (1:100), and anti-F4/80 Abs (Novus Biologicals, LLC, Centennial, CO, USA) (1:100) overnight at 4°C. After the washing step, the slides were stained with secondary donkey anti-rat IgG Abs conjugated with Alexa Fluor 488 (1:1,000) and donkey anti-rabbit IgG Abs conjugated with Alexa Fluor 546 (1:1,000) for 1 h in the dark at RT. They were mounted with Fluoroshield containing DAPI (Sigma-Aldrich, St. Louis, MO, USA). The stained slides were analyzed using a Carl-Zeiss confocal microscope LSM 700. For quantification, the mean fluorescence intensity (MFI) of Ly6G or F4/80 relative to DAPI was processed using ZEN 2.3 black software (Carl Zeiss, Dresden, Germany).

BALF protein and cytokine measurement

To measure BALF protein, BALF supernatant was collected after centrifugation. The supernatant was diluted by one-fifth and quantified by Pierce™ BCA Protein Assay Kit (ThermoFisher Scientific, Waltham, MA, USA). Cytokines were measured in the supernatant by using Duoset ELISA kits for mouse TNFα and VEGF (R&D Systems, Minneapolis, MN, USA) according to the manufacturer's protocol.

AM depletion and *in vivo* inhibitor treatment

To deplete AMs, mice were anesthetized and then intranasally pre-treated with clophosome A clodronate liposome (f70101c; FormuMax Scientific, Sunnyvale, CA, USA) 48 h before bacterial infection. Control mice were intranasally pre-treated with control liposome for clophosome (f70101; FormuMax Scientific). Mice were anesthetized and then intranasally treated with IgG control or anti-VEGF Ab (5 μg per mouse; R&D Systems) to block local alveolar VEGF at the same time as infection.

Flow cytometry and FACS sorting

Single cells from the dissociated lung or BALF pellet were lysed with RBC lysis buffer for 5 min at 4°C and centrifuged. After removing the supernatant, the cell pellet was washed twice with PBS containing 2% FBS. The washed pellet was counted using a hemocytometer and stained with Abs for 30 min at 4°C. The Abs were PE-Cy7-anti-CD45 (BD Bioscience, San Jose, CA, USA), eFlour-450-anti-Ly6G (eBioscience, San Diego, CA, USA), APC-anti-CD11c (BioLegend, San Diego, CA, USA), PE-anti-CD170 (SiglecF; BioLegend), FITC-anti-CD11b (BD Bioscience), Percp-cy5.5-anti-CD64 (BioLegend), and Brilliant-Violet711- anti-F4/80 (BioLegend). To examine *in vivo* AM cell death, BALF cells were stained with PE-cy7-anti-CD45, APC-anti-CD11c, PE-anti-CD170 (SiglecF), DAPI, and Annexin V-FITC Apoptosis Kit (BioVision Inc., Milpitas, CA, USA). The stained cells were analyzed using a FACS Fortessa BD flow cytometer. To isolate AMs, stained cells were isolated with $CD45^{+}CD11c^{+}SiglecF^{+}$ using BD FACS Aria II. The data was analyzed using FlowJo software (BD Biosciences).

MACS for $CD31^{+}$ endothelium and BMDN

The right lobes of the lung were chopped into small pieces and dissociated using a collagenase type II solution for 1 h at 37°C. The samples were filtered twice through a 70 μm strainer and washed. The single cells were washed after being processed in RBC lysis buffer for 5 min at 4°C. The single cells were stained with CD31 microbeads (130-097-418; Miltenyi Biotec, Bergisch Gladbach, Germany) for 20 min at 4°C. After washing, the stained samples were isolated by using positive selection in an autoMACS Pro separator (Miltenyi Biotec).

For BMDN sorting, the femurs and tibias of mice were removed and cut at both ends with scissors. A 5 ml of PBS was added, and the cells were lysed with RBC lysis buffer. The single cells were stained with a neutrophil isolation kit (130-097-658; Miltenyi Biotec) for 20 min at 4°C. After washing, the stained samples were isolated by using positive selection in an autoMACS Pro separator (Miltenyi Biotec).

Immunoblotting

Cells were lysed in RIPA buffer (Sigma-Aldrich) containing 1% Protease and Phosphatase Inhibitor Cocktail (Sigma-Aldrich) for 10 min on ice. The cells were sonicated and centrifuged for 15 min at 4 °C at 13,000 rpm. The supernatant was collected and quantified by Pierce™ BCA Protein Assay Kit (ThermoFisher Scientific). A total of 10 μg protein was loaded onto an 8% or 12% SDS-PAGE gel and then transferred to a polyvinylidene difluoride membrane by using a wet/tank transfer system (Bio-Rad, Hercules, CA, USA). The membrane was blocked by Tris-buffered saline with Tween 20 (TTBS) containing 5% Difco skim milk (BD Biosciences) for 1 h at room temperature. After blocking, the membrane was incubated with Purified anti-CD54 (ICAM1) Ab (BioLegend) or anti-VCAM1/CD106 Ab (R&D Systems) or anti-β-actin Ab (Santa Cruz Biotechnology, Santa Cruz, CA, USA) overnight at 4°C with rotation. The membrane was washed with TTBS three times and incubated with secondary Abs linked with HRP for 2 h at RT.

Real time PCR

Following MACS or FACS sorting, total mRNA was extracted from the isolated cells using GeneAll Hybrid-R (305-101; Geneall, Seoul, Korea). The extracted mRNA was quantified using a NANO DROP 1000 spectrophotometer (ThermoFisher Scientific). cDNA was obtained with PrimeScript RT Master Mix (RR036A; Takara, Kusatsu, Japan). Real-time PCR was performed with KAPA SYBR FAST (KK4605; Roche, Basel, Switzerland) and QuantStudio 3 Real-Time PCR System (Applied Biosystems, Waltham, MA, USA). The sequences were as follows: mouse NOX4 sense primer 5′-TTG CCT GGA AGA ACC CAA GT-3′, NOX4 antisense primer 5′-TCC GCA CAA TAA AGG CAC AA -3′, mouse ICAM1 sense primer 5′- AGG TGG TTC TTC TGA GCG GC-3′, ICAM1 antisense primer 5′-AAA CAG GAA CTT TCC CGC CA -3′, mouse GAPDH sense primer 5′-TAG GGC CTC TCT TGC TCA GT-3′, GAPDH antisense primer 5′-GGA CCT CAT GGC CTA CAT GG-3′. Gene specific expression was normalized against the GAPDH housekeeping gene. The relative expression was determined by the comparative $2^{-\Delta\Delta CT}$ method.

Ea.hy926 cell culture

Ea.hy926 cells were obtained from Yonsei University (Seoul, Korea) and maintained in Endothelial Cell Growth Medium-2 Bulletkit (EGM2, CC-3162; Lonza, Basel, Switzerland) at 37°C in a humidified 5% CO_2 incubator. Ea.hy926 cells in 6-well plates were pre-treated with 5 μM GLX353122 (HY-100111; MedChemExpress, Monmouth Junction, NJ, USA), a NOX4 inhibitor. The cells were treated for 6 h with 25 ng/ml recombinant human VEGF 165 ($rhVEGF_{165}$) at 37°C in a humidified 5% CO_2.

Ex vivo AM apoptosis assay

AMs ($CD45^+CD11c^+CD11b^-SiglecF^+$), isolated by FACS, were seeded and cultured *ex vivo* in DMEM (Lonza) in 12-well plates. The cells were infected with *S. aureus* (multiplicity of infection [MOI] 10) and incubated for 300 min at 37°C with 5% CO_2. They were then collected and stained using the Annexin V-FITC/PI Apoptosis Kit (BioVision Inc.). The stained cells were analyzed using a FACS Fortessa BD flow cytometer.

S. aureus-GFP uptake assay

BMDN isolated by MACS and AMs isolated by FACS were seeded in 12-well plates. The cells were infected with GFP-tagged *S. aureus* (MOI 10 or 20) and incubated for 1 h at 37°C with 5% CO_2. Then, they were collected in a tube and centrifuged at 4,000 rpm, 5 min, RT. The supernatant was cultivated on a BHI agar plate for measuring CFU. The pellet was washed twice and analyzed for GFP-positive populations using FACS as described previously.

Statistical analysis

Comparisons of 2 samples were processed by an unpaired Student's *t*-test, whereas analysis of variance was followed by one-way ANOVA using Bonferroni's multiple comparisons test in all statistical analyses. Comparisons of multiple samples, including time variance, were analyzed by two-way ANOVA test. Data were expressed as mean ± SEM for all graphs. p-values <0.05 were considered statistically significant. Statistical analyses were performed using the GraphPad PRISM 8 software (GraphPad, San Diego, CA, USA).

RESULTS

NOX4 is responsible for attenuation of lung inflammation at 24 h after *S. aureus* infection

To identify the immunologic role of NOX4 in bacterial lung infection, we examined the concentration of BALF proteins as a lung injury index in WT or NOX4 KO mice after *S. aureus* lung infection. In WT mice, BALF protein levels significantly increased at 12 h and then subsequently decreased until 120 h after infection. Conversely, in NOX4 KO mice, BALF protein levels exhibited a significant increase at 12 h, remained elevated at 24 h, and then decreased until 120 h after infection (**Fig. 1A**). Notably, although the levels in NOX4 KO mice were similar to those in WT mice at 12 h, they were three times higher than those in WT mice at 24 h (**Fig. 1A**). Furthermore, BALF protein levels showed a decline in WT mice after 12 h and in NOX4 KO mice after 24 h. Importantly, these levels tended to be higher in NOX4 KO mice than in WT mice from 48 h to 120 h after infection, although these differences did not reach statistical significance (**Fig. 1A**). To determine whether the lung injury in NOX4 KO mice was accompanied by an increased bacterial burden after infection, we quantified the number of remaining bacteria in BALF. The bacterial burden in BALF increased at 12 h and subsequently decreased until 120 h in WT mice (**Fig. 1B**). However, in contrast to the pattern of BALF protein levels, there was no discernible difference in bacterial burden between WT and NOX4 KO mice up to 120 h after infection (**Fig. 1B**). The levels of TNFα, a pro-inflammatory cytokine, increased at 12 h and subsequently decreased until 120 h in WT mice (**Fig. 1C**). Notably, at 24 h, TNFα levels were significantly higher in NOX4 KO mice than in WT mice (**Fig. 1C**). Therefore, these results showed that NOX4 KO mice had more inflammation than WT mice at 24 h after infection, and the increased inflammation was not derived from the difference in bacterial load.

Next, we investigated H&E staining images to identify the invasion of cells into the lung after *S. aureus* infection. The inflammatory score, based on H&E staining, indicated that immune cell infiltration in lung tissues peaked at 24 h after infection and then gradually decreased until 120 h in both WT and NOX4 KO mice (**Fig. 1D and E**). Moreover, NOX4 KO mice exhibited more extensive immune cell infiltration than WT mice at 24 h after infection (**Fig. 1D and E**). Furthermore, we performed immunofluorescence staining of neutrophils (Ly6G) and macrophages (F4/80) to examine the infiltrated cell types in the lung after infection (**Fig. 1F-H**). The immunofluorescence staining of neutrophils displayed a pattern similar to that observed in the H&E staining (**Fig. 1E and G**). At 24 h after infection, NOX4 KO mice exhibited significantly higher neutrophil infiltration into the lung compared to WT mice (**Fig. 1F and G**). However, the infiltration of macrophages was not as extensive as that of neutrophils, and there were no discernible differences between WT and NOX4 KO mice after infection (**Fig. 1F and H**). These results suggest that NOX4 is responsible for attenuation of neutrophilic inflammation at 24 h after *S. aureus* lung infection. Furthermore, the inflammation induced by *S. aureus* was resolved more rapidly in WT mice than in NOX4 KO mice from 24 to 120 h, implying that the absence of NOX4 delayed the resolution of inflammation.

NOX4 is responsible for AM recruitment at 24 h after *S. aureus* lung infection

Next, we examined the number of total cells in BALF in WT or NOX4 KO mice at 12 h and 24 h after *S. aureus* lung infection because NOX4 KO mice showed higher inflammation than WT mice at 24 h after infection. The number of cells in BALF increased in both WT and NOX4 KO mice at 12 h (**Fig. 2A**). Even though infiltrated cells in BALF were similar between WT and NOX4 KO mice at 12 h, the recruited cells in NOX4 KO mice were two times higher than those in WT

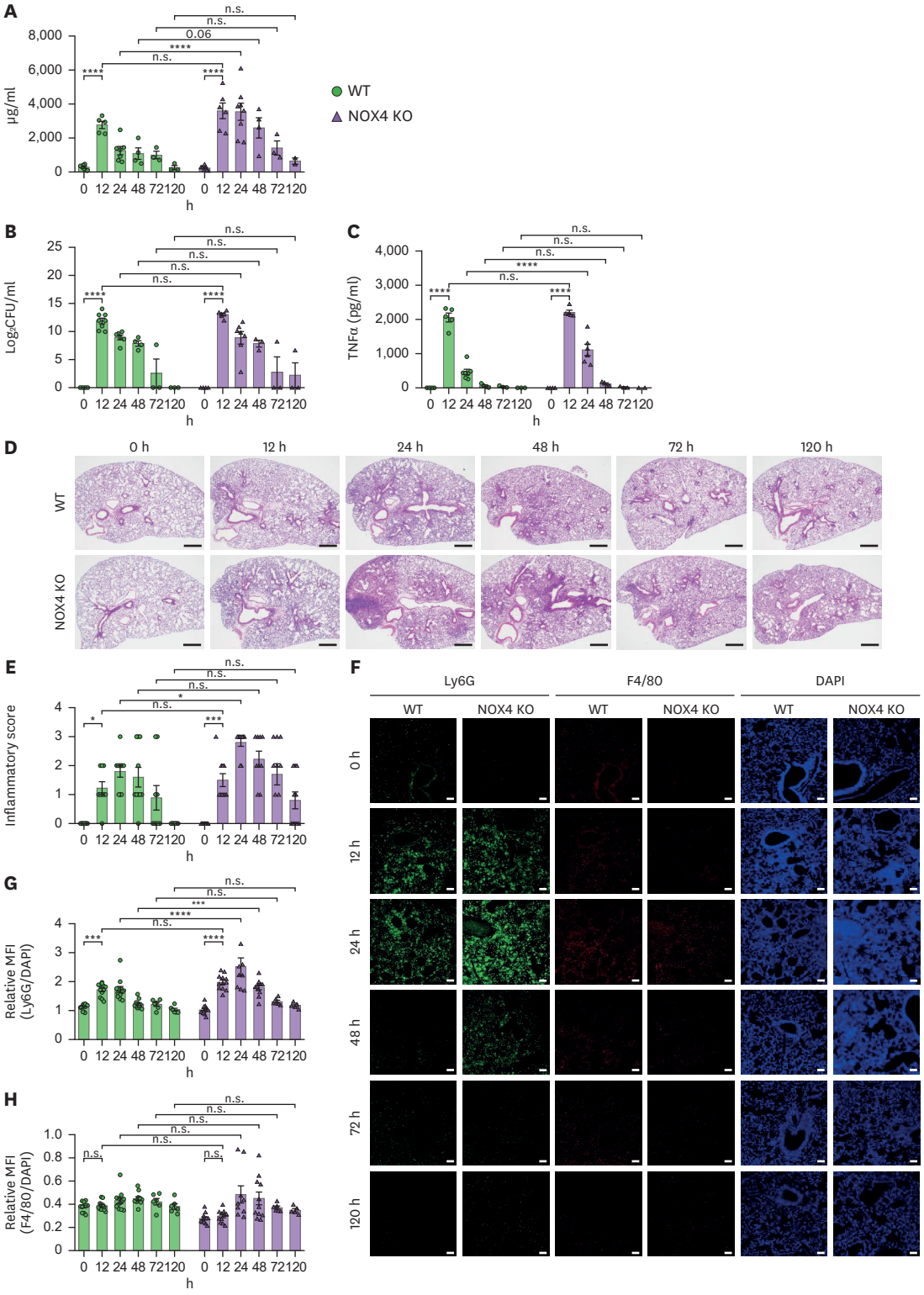

Figure 1. NOX4 is responsible for attenuation of lung inflammation at 24 h after *S. aureus* lung infection (n=2–9).
WT and NOX4 KO mice were intranasally infected with *S. aureus* (3×10^7 CFU) until 120 h. (A) Protein concentration in BALF after infection. (B) *S. aureus* CFU in the BALF. (C) Concentration of TNFα in the BALF. (D) Representative H&E images and (E) inflammatory scores of lung tissue (scale bar=500 μm). (F) Representative immunofluorescence staining images of Ly6G (green), F4/80 (red), and DAPI (blue). MFI of (G) Ly6G or (H) F4/80 relative to DAPI (scale bar=100 μm). All data were presented as mean ± SEM. The p-value using a two-way ANOVA (A-C, E, G, H).
*p<0.05, **p<0.01, ***p<0.001, ****p<0.0001.

https://doi.org/10.4110/in.2023.23.e42

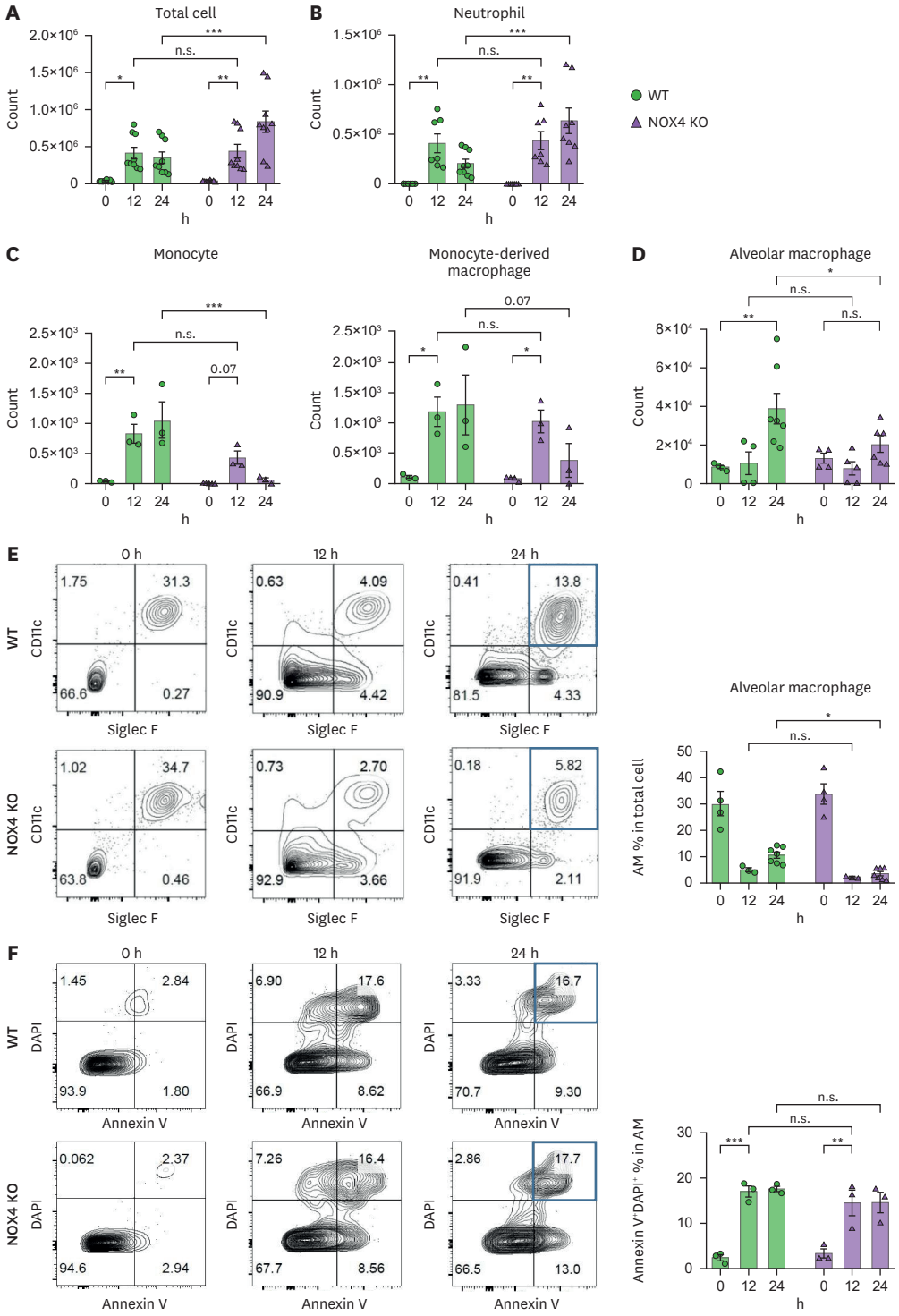

Figure 2. NOX4 is responsible for alveolar macrophage recruitment at 24 h after *S. aureus* lung infection (n=3–9).
WT and NOX4 KO mice were intranasally infected with *S. aureus* (3×10^7 CFU). (A) Total cell and (B) neutrophil counts ($CD45^+CD11b^+CD11c^-Ly6G^+$ $SiglecF^-$) in BALF. (C) Monocyte (left; $CD45^+CD11b^+CD11c^-Ly6G^-SiglecF^-CD64^+F4/80^-$) and monocyte-derived macrophage (right, $CD45^+CD11b^+CD11c^-Ly6G^-SiglecF^-CD64^+F4/80^+$) counts in BALF. (D) AM counts ($CD45^+CD11c^+SiglecF^+$). (E) Gate and percentages of AM in BALF. (F) Gate and Percentage of Annexin V^+DAPI^+ in AM gate ($CD45^+CD11c^+SiglecF^+$). The data showed three or more experiments, as in the symbol indicating individual mice. All data were presented as mean ± SEM. The p-value using a two-way ANOVA (A-F).
*p<0.05, **p<0.01, ***p<0.001, ****p<0.0001.

https://doi.org/10.4110/in.2023.23.e42

mice at 24 h (**Fig. 2A**). Next, we performed flow cytometry analysis to examine the infiltrated cell types in the BALF after infection (**Supplementary Fig. 1**). In BALF from NOX4 KO mice, the number of neutrophils is almost the same as that of total cells (**Fig. 2A and B**), and the percentage of neutrophils was almost 80% of total cells at 24 h after infection (**Supplementary Fig. 2A**). Moreover, the number of neutrophils in NOX4 KO mice was similar to that in WT mice at 12 h, whereas the cells in NOX4 KO mice were three times higher than those in WT mice at 24 h (**Fig. 2B**). Although the number of monocytes and monocyte-derived macrophages was too small compared to that of neutrophils, the number of these cells increased in WT mice at 12 and 24 h after infection (**Fig. 2C**). In contrast, in NOX4 KO mice, the number of these cells increased at 12 h but decreased at 24 h (**Fig. 2C**). Furthermore, NOX4 KO mice had a lower count of these cells than WT mice at 24 h after infection (**Fig. 2C**). However, the percentages of monocytes and monocyte-derived macrophages did not exhibit significantly increases at 12 h in either WT or NOX4 KO mice (**Supplementary Fig. 2B and C**). Nevertheless, at 24 h after infection, the percentages of these cells were lower in NOX4 KO mice than in WT mice (**Supplementary Fig. 2B and C**). These findings suggest that the neutrophil population is the main cellular type that is infiltrated in NOX4 KO mice's lungs, as well as that the neutrophil population is sustained in NOX4 KO mice at 24 h following infection.

AMs have been reported to be differentiated from monocytes (7) and to play an important role in the early host response to bacterial lung infections by regulating the inflammatory response, removing neutrophils, and promoting tissue repair (8,26). Therefore, we checked the number of AMs in WT or NOX4 KO mice at 12 and 24 h after *S. aureus* infection (**Fig. 2D**). The number of AMs in BALF was similar between WT and NOX4 KO mice in the absence of infection. At 12 h after infection, the number of AMs in both WT and NOX4 KO mice was almost the same. Interestingly, the number of AMs decreased in NOX4 KO mice compared to that in WT mice at 24 h after infection (**Fig. 2D**). Following infection, the total cell count in BALF increased due to inflammation, mainly attributed to the recruitment of neutrophils (**Fig. 2A and B**, **Supplementary Fig. 2A**). Consequently, the percentage of AMs in BALF appeared to decrease at 12 and 24 h after infection (**Fig. 2E**). Although it may appear that the percentage of AMs decreases at 12 and 24 h, it was significantly lower in NOX4 KO mice than in WT mice at 24 h after infection (**Fig. 2E**). To investigate the cause of the reduction of AMs in NOX4 KO mice after infection, we examined *in vivo* flow cytometry-based apoptosis analysis (Annexin V & DAPI) in AM population. The percentage of necrotic cells (Annexin V^+ $DAPI^+$) in AMs increased in WT mice at 12 and 24 h after infection (**Fig. 2F**). The percentage of necrotic cells in AMs was comparable between WT and NOX4 KO mice at 12 and 24 h after infection (**Fig. 2F**). Therefore, the reduction of AM in NOX4 KO mice at 24 h after infection was not due to increasing cell death. These results indicated that NOX4 is responsible for AM recruitment into the lung at 24 h after *S. aureus* lung infection. Moreover, the increased level of lung injury and neutrophil number in NOX4 KO mice at 24 h after *S. aureus* infection may be attributed to the decreased level of AMs in NOX4 KO mice at 24 h after infection.

NOX4 is not involved in the antibacterial activity of neutrophils and AMs upon *S. aureus* infection

We questioned whether intrinsic NOX4 affected the function of neutrophils after *S. aureus* infection. To investigate the phagocytic capacity of neutrophils, we isolated bone-marrow derived neutrophils (BMDN) from WT or NOX4 KO mice using MACS. In BMDN from WT and NOX4 KO mice, there were no differences in the uptake of GFP-tagged *S. aureus* at different time points within 1 h (**Fig. 3A**). The percentages of apoptotic and necrotic cell death were also similar in both WT and NOX4 KO BMDN after GFP-tagged *S. aureus* infection (**Fig. 3B and C**).

https://doi.org/10.4110/in.2023.23.e42

Moreover, BMDN isolated from both WT and NOX4 KO mice exhibited similar bacterial killing ability with MOI 5 or 20 at 30 min (**Fig. 3D**).

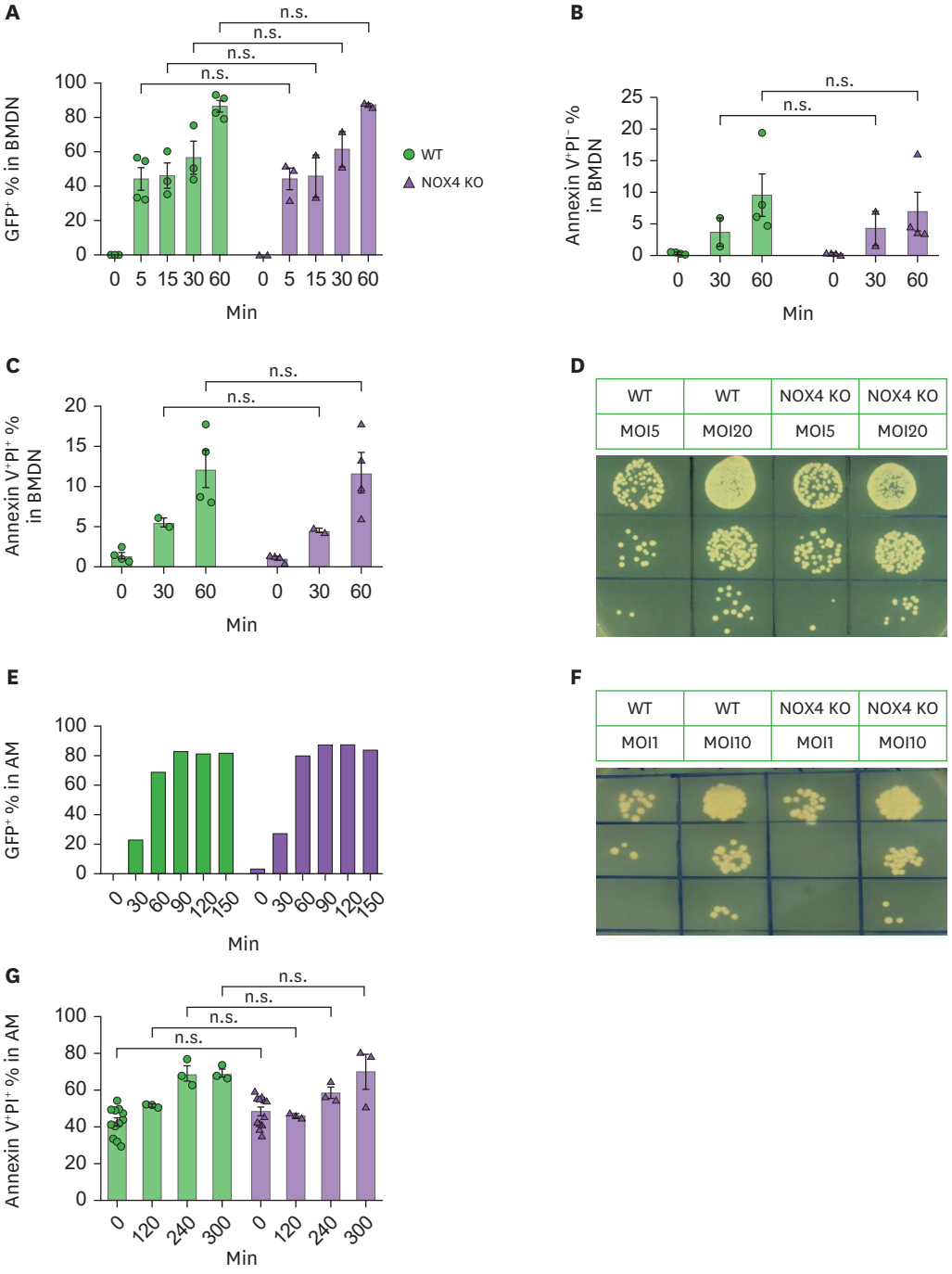

Figure 3. NOX4 is not involved in the antibacterial activity of neutrophils and AMs upon *S. aureus* infection.
(A-D) *Ex vivo* BMDNs from WT or NOX4 KO mice were infected with *S. aureus* at the indicated time point. (A) Percentages of GFP⁺ BMDNs with MOI 10. (B) Percentages of apoptotic cells (Annexin V⁺PI⁻) in BMDNs with MOI 10. (C) Percentage of necrotic cells (Annexin V⁺PI⁺) in BMDNs with MOI 10. (D) *S. aureus* CFU in media with MOI 5 or 20 at 30 min after infection. (E-G) *Ex vivo* AMs from WT or NOX4 KO mice were infected with *S. aureus*. (E) Percentages of GFP⁺ AMs after infection with MOI 1. (F) *S. aureus* CFU in media at 60 min after infection with MOI 1 or 10. (G) Percentage of necrotic cells (Annexin V⁺PI⁺) in AMs with MOI 10. All data were presented as mean ± SEM. Two-way ANOVA (A-C, G).

https://doi.org/10.4110/in.2023.23.e42

Next, we investigated whether intrinsic NOX4 directly influenced the function of AMs after infection. To examine the phagocytic capacity and killing ability of AMs, we isolated them from WT or NOX4 KO mice using FACS. AMs from WT or NOX4 KO mice showed similar patterns in bacterial uptake and bacterial killing ability at different time points and doses (**Fig. 3E and F**). Additionally, we conducted *ex vivo* flow cytometry-based apoptosis analysis (Annexin V & PI) in AMs with *S. aureus* (MOI 10). AMs isolated from WT or NOX4 KO mice exhibited that no significant differences in necrotic cell death in response to *S. aureus* infection (**Fig. 3G**). These findings suggest that intrinsic NOX4 has no discernible effect on neutrophil and AM function, including antibacterial activity and cell death, in response to *S. aureus* infection.

NOX4 is necessary to induce ICAM1 expression on endothelial cells after *S. aureus* infection

Given that NOX4 is not intrinsically involved in the antibacterial activity of neutrophils and AMs, we hypothesized that NOX4 could operate in cells other than neutrophils and AMs to control their numbers upon *S. aureus* infection. Since NOX4 is reported to be expressed in lung endothelial cells (19,22), and lung endothelium is responsible for monocyte recruitment from blood to alveoli (5,27), we focused on the role of NOX4 in lung endothelial cells upon *S. aureus* infection. We isolated lung $CD31^+$ endothelial cells from WT or NOX4 KO mice using MACS and examined the expression of NOX4 after *S. aureus* infection. In the WT endothelial cell, we observed a significant increase in NOX4 gene expression at 12 h, followed by a decrease at 24 h after infection (**Fig. 4A**). To investigate whether NOX4 in endothelial cells could be involved in the recruitment of AMs into the lung after infection, we examined the expression level of endothelial adhesion molecules such as ICAM1 which are known to play an important role in monocyte recruitment on endothelial cells (5,27). The level of ICAM1 mRNA expression in WT mice endothelial cells increased at 12 h and decreased at 24 h after *S. aureus* infection (**Fig. 4B**), which were similar patterns to NOX4 expression (**Fig. 4A**). Interestingly, the mRNA expression level of ICAM1 in endothelial cells from NOX4 KO mice was lower than that in endothelial cells from WT mice at 12 h after infection (**Fig. 4B**). Similar to the alteration pattern of mRNA expression, the protein level of ICAM1 in NOX4 KO mice endothelial cells was lower than that in WT mice endothelial cells at 12 h after infection (**Fig. 4C**). The protein level of vascular cell adhesion molecule-1 was also known to be associated with monocyte recruitment (6,28). However, there was no difference in the protein level of VCAM1 in the endothelial cells from WT and NOX4 KO mice after infection (**Fig. 4C**). Taken together, we showed that NOX4 is necessary to induce the expression of ICAM1, but not VACM1, in endothelial cells upon *S. aureus* infection, suggesting that NOX4 might induce recruitment of AMs by controlling ICAM1 expression in lung endothelial cells.

Previous studies have reported that VEGF can induce ICAM1 expression in various endothelial cells (29-31), and that NOX4 colocalizes with and interacts with a VEGF receptor 2 (VEGFR2) in the endothelium (32). Furthermore, NOX4 can stabilize VEGFR2 and promote endothelial cell function (33). These reports suggest that VEGF may regulate NOX4-mediated ICAM1 expression in endothelial cells after *S. aureus* infection. Thus, we investigate whether VEGF regulates the ICAM1 expression by NOX4. We first inactivated NOX4 activity using GLX351322, NOX4 inhibitor, in a stable human endothelial cell line such as Ea.hy926 cells. We next measured ICAM1 expression at 3 and 6 h after treatment with $rhVEGF_{165}$ in the presence or absence of GLX35122. At 6 h after $rhVEGF_{165}$ treatment, ICAM1 expression increased, and increased ICAM1 expression was reduced by GLX35122 treatment (**Fig. 4D**), indicating that VEGF can induce endothelial ICAM1 expression in a NOX4-dependent manner.

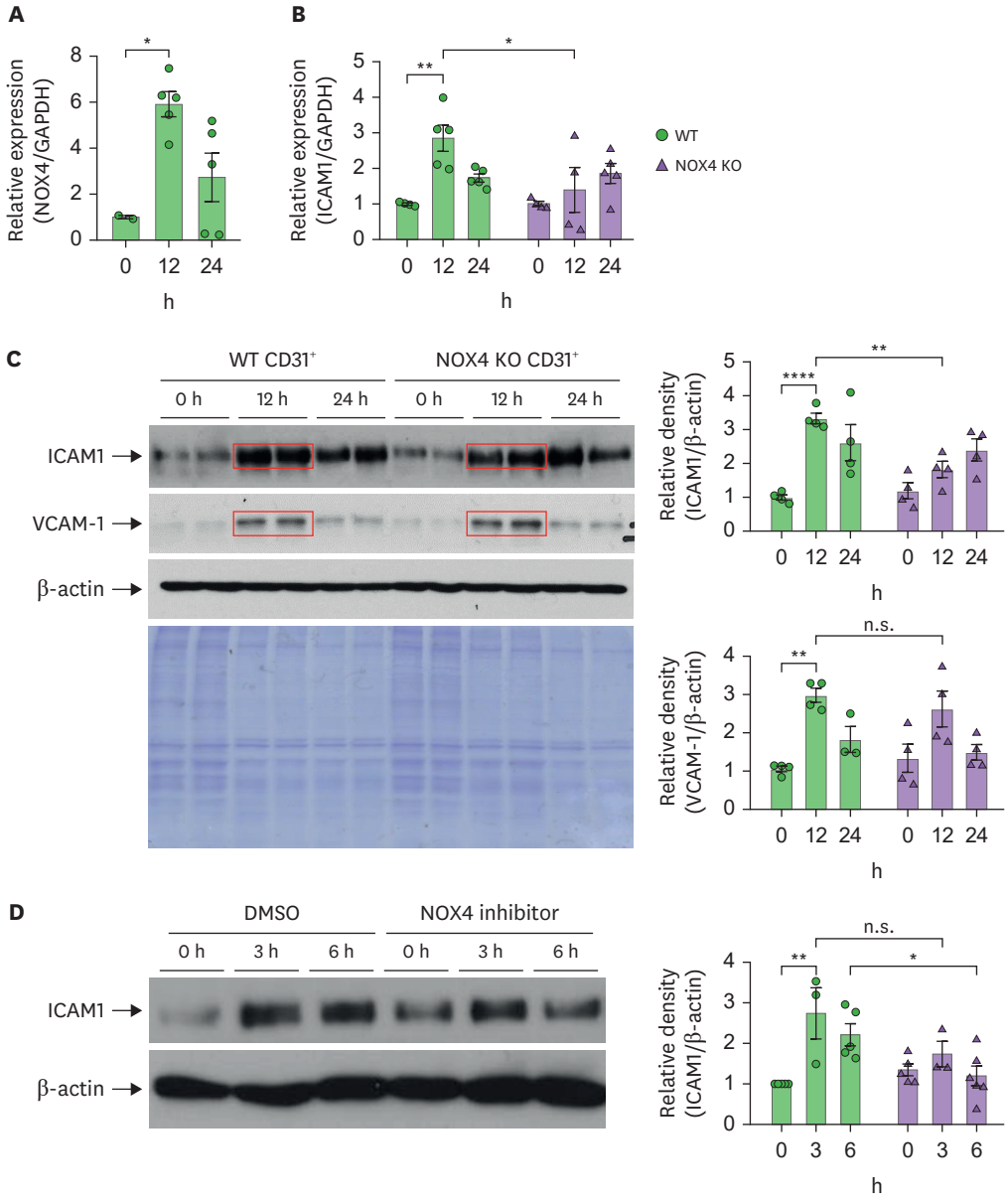

Figure 4. NOX4 is necessary to induce ICAM1 expression on endothelial cells after *S. aureus* infection (n=3–5).
(A-C) CD31⁺ endothelial cells were isolated using MACS from WT or NOX4 KO mice lungs at 0, 12, and 24 h after *S. aureus* infection. (A) Expression of NOX4 mRNA in CD31⁺ endothelial cells. (B) Expression of ICAM1 mRNA in endothelial cells by real-time PCR. (C) Immunoblot of ICAM1, VCAM-1, β-actin, and Coomassie staining. Representative image (left) and relative density quantified from immunoblot (right). (D) Ea.hy926 cells were pretreated with 10 μM GLX351322 to inhibit NOX4 prior to $rhVEGF_{165}$ treatment. Immunoblot of ICAM1. Representative image (left) and relative density quantified from immunoblot (right). All data were presented as mean ± SEM. The p-value using a one-way ANOVA (A) and two-way ANOVA (B-D).
*p<0.05, **p<0.01, ****p<0.0001.

VEGF attenuates lung inflammation via inducing AM recruitment after *S. aureus* infection

We wondered whether VEGF is induced in WT mice upon *S. aureus* infection. Therefore, we examined the concentration of VEGF in BALF after *S. aureus* infection. We found that the level of VEGF was increased at 12 h and decreased at 24 h after lung infection in WT mice (**Fig. 5A**). In addition, the increased level of VEGF in NOX4 KO mice was almost the same as that in WT mice (**Fig. 5A**), indicating that VEGF is increased upon *S. aureus* infection in a NOX4-independent manner.

https://doi.org/10.4110/in.2023.23.e42

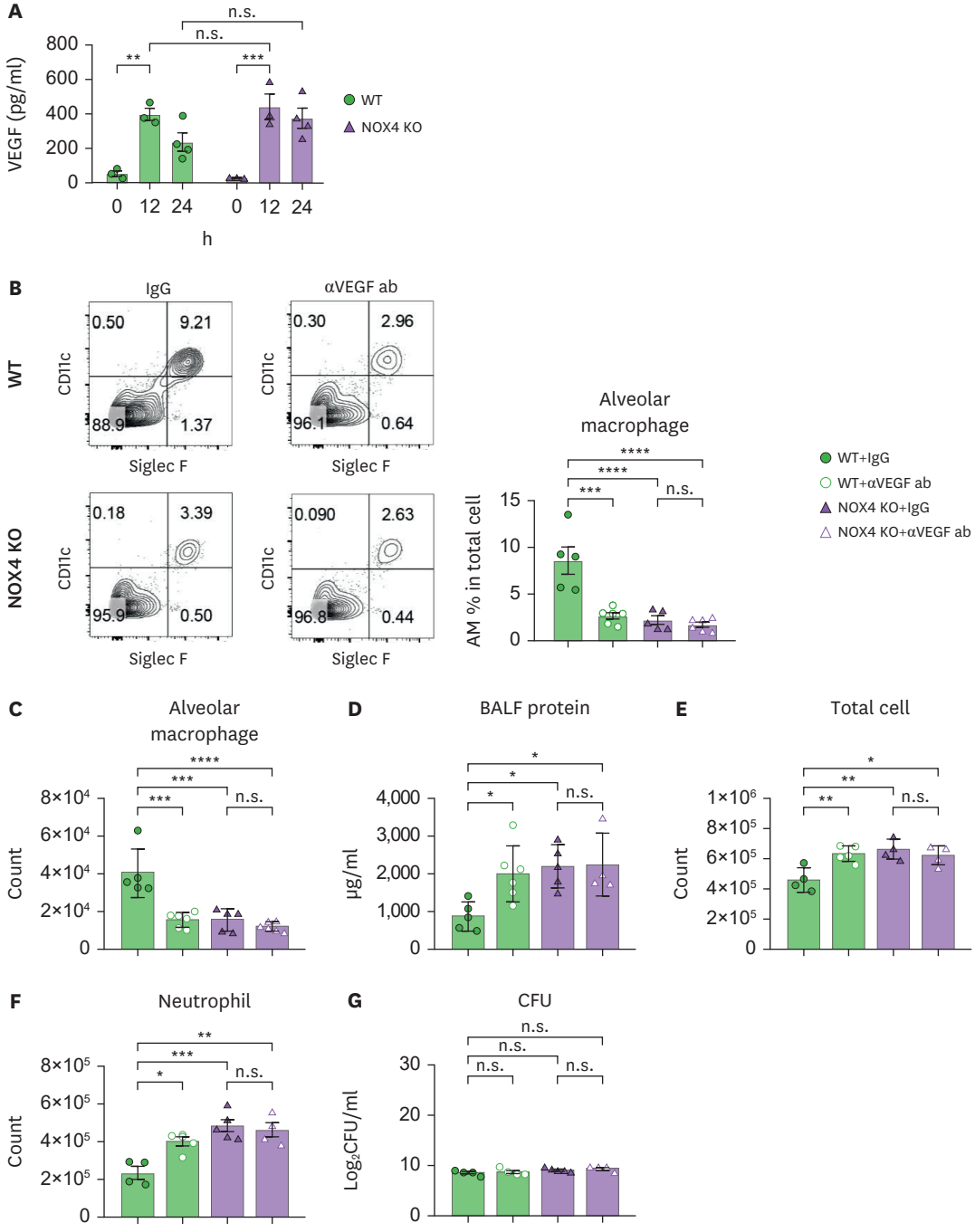

Figure 5. VEGF attenuates lung inflammation via inducing AM recruitment at 24 h after *S. aureus* lung infection (n=3–6).
(A) VEGF concentration in BALF from WT and NOX4 KO mice. (B-G) WT and NOX4 KO mice intranasally treated with IgG or anti-VEGF Abs, and they were infected with 3×10^7 CFU of *S. aureus* at the same time. The inflammatory responses were assessed at 24 h after the infection. (B) Representative flow cytometry plots (left), and percentages of AM in total BALF cell (right). (C) AM counts in BALF. (D) Protein concentration in BALF. (E) Total cell counts in BALF. (F), neutrophil counts in BALF. (G) *S. aureus* CFU in BALF. The data showed 3 experiments, with the symbol representing individual mice. All data were presented as mean ± SEM. The p-value using two-way ANOVA (A) and one-way ANOVA (B-G).
*p<0.05, **p<0.01, ***p<0.001, ****p<0.0001.

Next, we investigated the functional role of VEGF in AM recruitment upon *S. aureus* infection. To test this, we intranasally treated WT and NOX4 KO mice with anti-VEGF Abs together with *S. aureus* to block local VEGF in alveoli. We then examined the ratio and number of AMs

https://doi.org/10.4110/in.2023.23.e42

in BALF at 24 h post-infection in the presence of control IgG or anti-VEGF Abs. Anti-VEGF treatment significantly reduced the ratio and number of AMs in WT mice, which were similar to those in IgG-treated NOX4 KO mice (**Fig. 5B and C**). Furthermore, the ratio and number of AMs in IgG-treated NOX4 KO mice did not differ from those in anti-VEGF-treated NOX4 KO mice (**Fig. 5B and C**). These results suggest that VEGF, increased by *S. aureus* infection, can recruit AMs in NOX4-dependent manner. In this context, we wondered whether increased VEGF is responsible for the attenuation of neutrophilic inflammation and lung injury upon *S. aureus* infection. Anti-VEGF treatment increased the levels of BALF protein (**Fig. 5D**), BALF cells (**Fig. 5E**), and neutrophils (**Fig. 5F**) in WT mice, which were similar to those in IgG- or anti-VEGF-treated NOX4 KO mice (**Fig. 5D-F**). However, bacterial loads were not affected in all groups (**fig. 5G**). Taken together, our results demonstrate that VEGF in the alveoli is essential for protecting against *S. aureus* infection by recruiting AMs in NOX4-dependent manner.

NOX4 attenuates lung inflammation via inducing AM recruitment after *S. aureus* infection

To investigate the functional role of AMs in neutrophilic inflammation and lung injury upon *S. aureus* infection, we intranasally treated mice with clodronate liposome to deplete AMs at 48 h prior to *S. aureus* infection (34). Clodronate liposome treatment significantly reduced the ratio and number of AMs in WT mice, similar to those in isotype liposome-treated NOX4 KO mice (**Fig. 6A and B**). Moreover, the ratio and number of AMs in isotype liposome-treated NOX4 KO mice were not different from those in clodronate liposome-treated NOX4 KO mice (**Fig. 6A and B**). Clodronate liposome treatment increased the levels of BALF protein (**Fig. 6C**), BALF cells (**Fig. 6D**), and neutrophils (**Fig. 6E**) in WT mice, similar to those in isotype liposome- or clodronate liposome-treated NOX4 KO mice (**Fig. 6C-E**). However, bacterial loads were not affected in all groups (**Fig. 6F**). These results demonstrate that AM recruitment is required for the resolution of neutrophilic inflammation in a NOX4-dependent manner after *S. aureus* infection.

In this study, *S. aureus* lung infection simulates the production of VEGF in alveoli. When NOX4 is present, the elevated VEGF levels induce endothelial ICAM1 expression in a NOX4-dependent manner, facilitating the recruitment of AMs to the alveoli. These recruited AMs play a crucial role in reducing neutrophilic inflammation. However, in the absence of NOX4, increased VEGF is unable to significantly enhance endothelial ICAM1 expression, leading to insufficient recruitment of AMs to the alveoli. This deficiency in AMs results in excessive neutrophilic inflammation (**Fig. 7**).

DISCUSSION

Our study found that *S. aureus* infection resulted in higher levels of neutrophil infiltration and lung injury in NOX4 KO mice compared to WT mice, indicating a protective role for NOX4 in the host response. NOX4 is a protein involved in both the production and sensing of ROS in various types of cells, including endothelial cells (35,36), epithelial cells (37,38), and monocytes (39,40). NOX4 has been demonstrated to play a dual function in lung infections in different cell types. It can either contribute to or reduce host damage. For instance, following *P. aeruginosa* infection, NOX4 was found to increase nuclear ROS and trigger chromatin remodeling in lung epithelial cells, leading to host injury (41). On the other hand, NOX4-mediated ROS has been reported to promote the production of macrophage migration inhibitory factor, which aids in resisting *T. gondii*, indicating a protective role for NOX4 in the

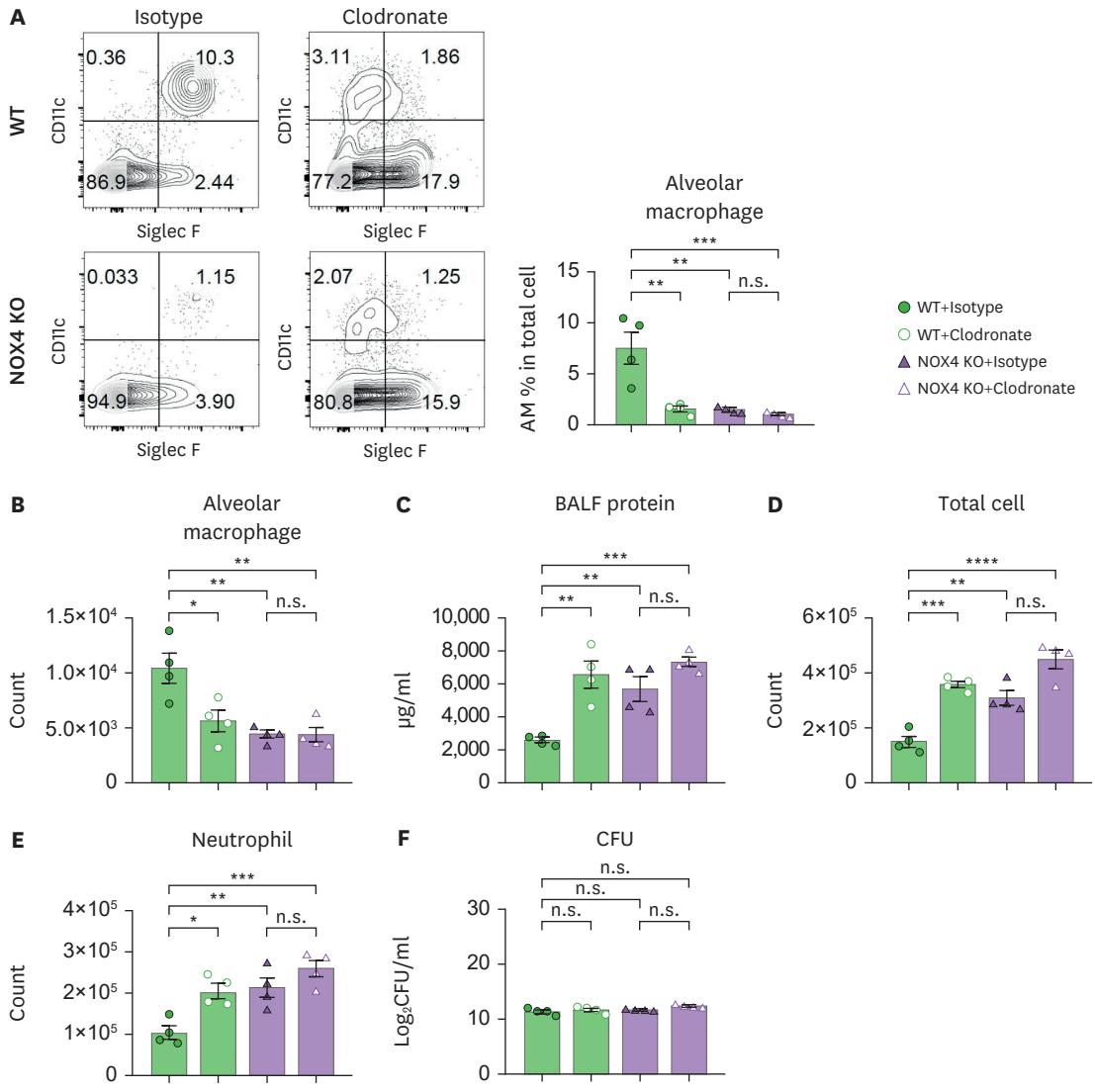

Figure 6. NOX4 attenuates lung inflammation via inducing AM recruitment at 24 h after *S. aureus* lung infection (n=4–6).
WT and NOX4 KO mice were intranasally administrated with clodronate liposome or isotype liposome 48 h before *S. aureus* infection. They were infected with *S. aureus* (3×10^7 CFU) and sacrificed after 24 h. (A) Representative flow-cytometry plots (left), and percentages of AM in BALF cells (right). (B) AM counts in BALF. (C) Protein concentration in BALF. (D) Total cell counts and (E) neutrophil counts in BALF. (F) *S. aureus* CFU in BALF. The data showed two or more experiments, as in the symbol indicating individual mice. Bars represented means ± SEM. The p-value using one-way ANOVA was used for (A-F).
*p<0.05, **p<0.01, ***p<0.001, ****p<0.0001.

host (24). Thus, our study provides evidence supporting the protective role of endothelial NOX4 in the host during lung infection. The role of NOX4 in the immune response after infection has been a topic of debate in previous studies, and although its function has been examined in response to various pathogens, its interaction with endothelial NOX4 and *S. aureus* has not been explored until our study. Therefore, we discovered a novel finding: endothelial NOX4 plays a role in reducing lung injury after *S. aureus* infection. Nevertheless, more research is required using specific conditional KO mice for NOX4 deletion in endothelial cells to fully comprehend the immunological function of endothelial NOX4 against *S. aureus* infection.

Endothelial ICAM1 is an adhesion molecule that is responsible for the recruitment of monocytes and neutrophils (28,42-44). Monocyte recruitment is dependent on ICAM1

https://doi.org/10.4110/in.2023.23.e42

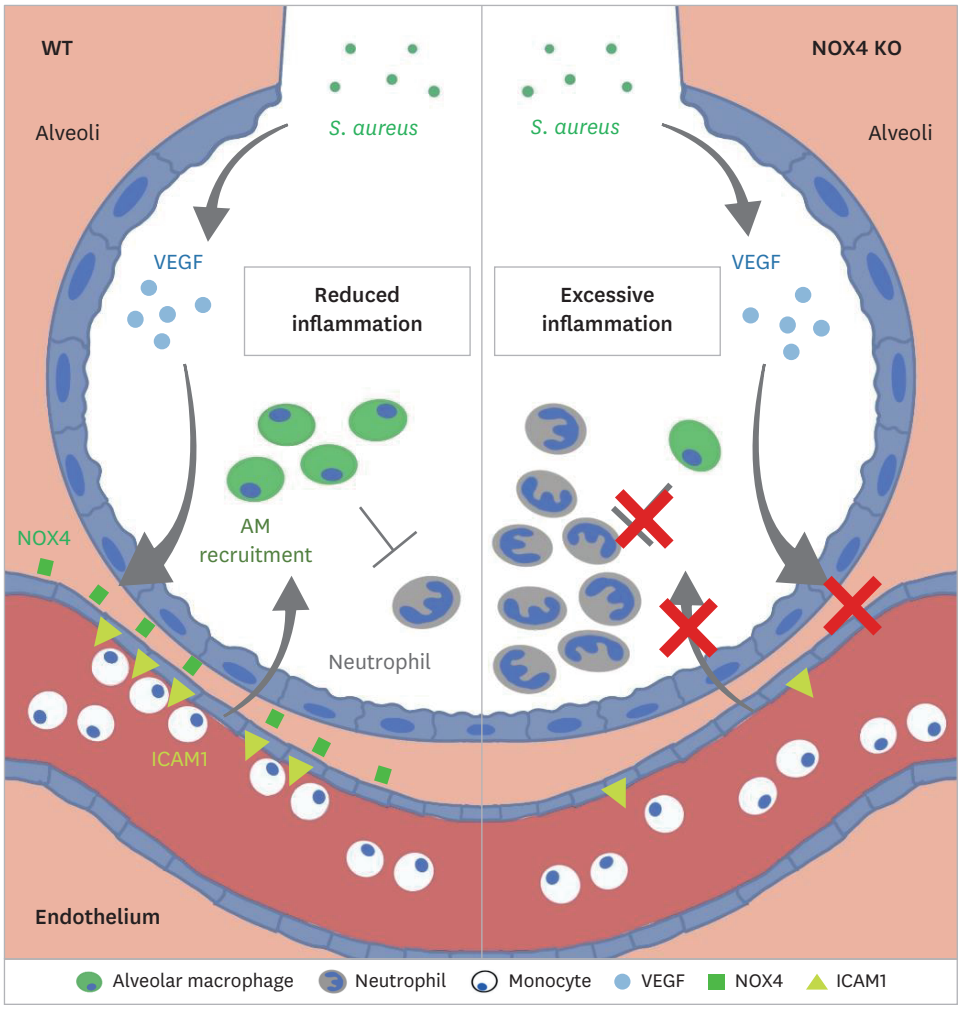

Figure 7. Schematic of the study.
S. aureus lung infection triggers the production of VEGF in the alveoli. In WT mice, elevated levels of VEGF can stimulate the expression of endothelial ICAM1 in a NOX4-dependent manner. Consequently, the AMs were recruited to the alveoli through the increased endothelial ICAM1, and they reduced neutrophilic inflammation. However, in NOX4 KO mice, the increased VEGF is not able to induce appropriate endothelial ICAM1 expression, resulting in insufficient AM recruitment in the alveoli. As a result, the insufficient AMs cause excessive neutrophilic inflammation.

expression in endothelial cells in response to specific pathogen or stimuli (42). Moreover, N-glycosylation of endothelial ICAM1 has been shown to influence the recruitment of specific monocyte subsets to sites of inflammation (45,46). Specifically, high mannose ICAM1 exhibits a selective function in binding to $CD16^{+}$ monocytes, while not interacting with $CD16^{-}$ monocytes or neutrophils (5). Furthermore, NOX4 has been associated with inducing specific binding between ICAM1 and monocytes in endothelial cells (22,28). These studies lend support to our results and hypothesis that NOX4 induces ICAM1 expression and may modify the glycosylated structures on ICAM1. Such modifications could potentially create a distinct binding site for monocytes or monocyte-derived macrophages rather than neutrophils, although we did not investigate the NOX4-dependent N-glycosylation state of ICAM1 in our mouse model. In our study, TNFα expression in BALF was higher in NOX4 KO mice than in WT mice at 24 h after *S. aureus* infection, coinciding with the same time points at which neutrophil recruitment increased in NOX4 KO mice. Considering that TNFα serves as a

https://doi.org/10.4110/in.2023.23.e42

potent chemoattractant for neutrophil recruitment into the lungs following bacterial infection (47,48), and that TNFα is not the primary cytokine responsible for AM recruitment during bacterial lung infection, the heightened neutrophil recruitment observed in NOX4 KO mice at 24 h may be attributed to the increased levels of TNFα or certain unidentified chemokines.

Furthermore, our study demonstrated that the AMs were required to repair the lung injury after *S. aureus* infection. We used AM depletion to show that the absence of AMs resulted in more severe lung inflammation and tissue damage in WT mice. AMs resolve lung inflammation and repair tissue damage (8) by up-regulating matrix metallopeptidases, which are involved in tissue remodeling (49). Previous research has indicated that AMs are proficient in phagocytosing neutrophils recruited during pathogenic infections, utilizing scavenging receptors like CD204 or surfactant protein A (50,51). Additionally, the effective clearance of recruited apoptotic neutrophils by AMs plays a pivotal role in ameliorating inflammation stemming from bacterial or influenza virus infections (51-53). These findings collectively suggest that AMs may alleviate excessive inflammation and promote resolution by eliminating infiltrated lung neutrophils following pathogenic infections, thus contributing to tissue repair. In our study, NOX4 KO mice exhibited more pronounced neutrophilic inflammation than WT mice. However, in the context of AM depletion, both WT and NOX4 KO mice displayed similar levels of neutrophilic inflammation post-infection. Although the precise mechanisms underlying how AMs regulate inflammation following *S. aureus* infection remain elusive, these results imply that the increased abundance of AMs in WT mice potentially plays a role in resolving excessive inflammation following *S. aureus* infection.

Previously, it has been reported that AMs are characterized as tissue-resident AMs or monocyte-derived AMs (54). In states of infection or injury, resident AMs are immediately infiltrated by recruited monocyte-derived AMs that integrate into the alveoli by transmigration and differentiation, and these resident and recruited AMs play a role in resolving infection and repairing the lung (55,56). Although our study did not determine the origin of AMs, we demonstrated that the recruited AMs were necessary for the resolution of inflammation after *S. aureus* infection.

In this study, we demonstrated that the presence of NOX4 is necessary to induce ICAM1 expression in lung endothelial cells after *S. aureus* infection through VEGF, which subsequently leads to the recruitment of AMs. These recruited AMs play a crucial role in reducing neutrophilic inflammation. Our findings suggest that NOX4 and its downstream signaling pathways play a crucial role in orchestrating the recruitment of AMs to resolve neutrophilic inflammation in response to *S. aureus* infection. These results provide new insights into the development of novel therapeutic strategies for lung infections caused by *S. aureus*.

ACKNOWLEDGEMENTS

This work was supported by the Bio & Medical Technology Development Program of the National Research Foundation of Korea (NRF) funded by the Ministry of Science, ICT & Future Planning (2019M3A9B6066971 to J.-H.R.), and the Korea Mouse Phenotyping Project (2016M3A9D5A01952415 to J.-H.R.). This study was supported by a faculty research grant of Yonsei University College of Medicine (6-2017-0075 to J.-H.R.). We would like to thank Sang Sun Yoon (Yonsei University, Korea) for providing GFP-tagged *S. aureus*; In-Hong Choi (Yonsei University, Korea) for providing Ea.hy926 cell.

SUPPLEMENTARY MATERIALS

Supplementary Figure 1

The gating strategy for isolating immune cells in BALF.

Click here to view

Supplementary Figure 2

The frequency of immune cells in BALF after *S. aureus* lung infection (n=3).

Click here to view

REFERENCES

1. Aberdein JD, Cole J, Bewley MA, Marriott HM, Dockrell DH. Alveolar macrophages in pulmonary host defence the unrecognized role of apoptosis as a mechanism of intracellular bacterial killing. *Clin Exp Immunol* 2013;174:193-202.
PUBMED | CROSSREF
2. Hussell T, Bell TJ. Alveolar macrophages: plasticity in a tissue-specific context. *Nat Rev Immunol* 2014;14:81-93.
PUBMED | CROSSREF
3. Mathie SA, Dixon KL, Walker SA, Tyrrell V, Mondhe M, O'Donnell VB, Gregory LG, Lloyd CM. Alveolar macrophages are sentinels of murine pulmonary homeostasis following inhaled antigen challenge. *Allergy* 2015;70:80-89.
PUBMED | CROSSREF
4. Shi C, Pamer EG. Monocyte recruitment during infection and inflammation. *Nat Rev Immunol* 2011;11:762-774.
PUBMED | CROSSREF
5. Regal-McDonald K, Xu B, Barnes JW, Patel RP. High-mannose intercellular adhesion molecule-1 enhances CD16$^+$ monocyte adhesion to the endothelium. *Am J Physiol Heart Circ Physiol* 2019;317:H1028-H1038.
PUBMED | CROSSREF
6. Lin YT, Chen LK, Jian DY, Hsu TC, Huang WC, Kuan TT, Wu SY, Kwok CF, Ho LT, Juan CC. Visfatin promotes monocyte adhesion by upregulating ICAM-1 and VCAM-1 expression in endothelial cells via activation of p38-PI3K-Akt signaling and subsequent ROS production and IKK/NF-κb activation. *Cell Physiol Biochem* 2019;52:1398-1411.
PUBMED | CROSSREF
7. McQuattie-Pimentel AC, Budinger GR, Ballinger MN. Monocyte-derived alveolar macrophages: the dark side of lung repair? *Am J Respir Cell Mol Biol* 2018;58:5-6.
PUBMED | CROSSREF
8. Allard B, Panariti A, Martin JG. Alveolar macrophages in the resolution of inflammation, tissue repair, and tolerance to infection. *Front Immunol* 2018;9:1777.
PUBMED | CROSSREF
9. Das A, Sinha M, Datta S, Abas M, Chaffee S, Sen CK, Roy S. Monocyte and macrophage plasticity in tissue repair and regeneration. *Am J Pathol* 2015;185:2596-2606.
PUBMED | CROSSREF
10. Westphalen K, Gusarova GA, Islam MN, Subramanian M, Cohen TS, Prince AS, Bhattacharya J. Sessile alveolar macrophages communicate with alveolar epithelium to modulate immunity. *Nature* 2014;506:503-506.
PUBMED | CROSSREF
11. Jain S, Williams DJ, Arnold SR, Ampofo K, Bramley AM, Reed C, Stockmann C, Anderson EJ, Grijalva CG, Self WH, et al. Community-acquired pneumonia requiring hospitalization among U.S. children. *N Engl J Med* 2015;372:835-845.
PUBMED | CROSSREF
12. Ryu JC, Kim MJ, Kwon Y, Oh JH, Yoon SS, Shin SJ, Yoon JH, Ryu JH. Neutrophil pyroptosis mediates pathology of *P. aeruginosa* lung infection in the absence of the NADPH oxidase NOX2. *Mucosal Immunol* 2017;10:757-774.
PUBMED | CROSSREF

13. Self WH, Wunderink RG, Williams DJ, Zhu Y, Anderson EJ, Balk RA, Fakhran SS, Chappell JD, Casimir G, Courtney DM, et al. *Staphylococcus aureus* community-acquired pneumonia: prevalence, clinical characteristics, and outcomes. *Clin Infect Dis* 2016;63:300-309.
PUBMED | CROSSREF

14. Buvelot H, Posfay-Barbe KM, Linder P, Schrenzel J, Krause KH. *Staphylococcus aureus*, phagocyte NADPH oxidase and chronic granulomatous disease. *FEMS Microbiol Rev* 2017;41:139-157.
PUBMED | CROSSREF

15. Wertheim HF, Melles DC, Vos MC, van Leeuwen W, van Belkum A, Verbrugh HA, Nouwen JL. The role of nasal carriage in *Staphylococcus aureus* infections. *Lancet Infect Dis* 2005;5:751-762.
PUBMED | CROSSREF

16. Parker D, Prince A. Immunopathogenesis of *Staphylococcus aureus* pulmonary infection. *Semin Immunopathol* 2012;34:281-297.
PUBMED | CROSSREF

17. DeLeo FR, Diep BA, Otto M. Host defense and pathogenesis in *Staphylococcus aureus* infections. *Infect Dis Clin North Am* 2009;23:17-34.
PUBMED | CROSSREF

18. Bernard K, Hecker L, Luckhardt TR, Cheng G, Thannickal VJ. NADPH oxidases in lung health and disease. *Antioxid Redox Signal* 2014;20:2838-2853.
PUBMED | CROSSREF

19. Basuroy S, Tcheranova D, Bhattacharya S, Leffler CW, Parfenova H. Nox4 NADPH oxidase-derived reactive oxygen species, via endogenous carbon monoxide, promote survival of brain endothelial cells during TNF-α-induced apoptosis. *Am J Physiol Cell Physiol* 2011;300:C256-C265.
PUBMED | CROSSREF

20. Martyn KD, Frederick LM, von Loehneysen K, Dinauer MC, Knaus UG. Functional analysis of NOX4 reveals unique characteristics compared to other NADPH oxidases. *Cell Signal* 2006;18:69-82.
PUBMED | CROSSREF

21. Pendyala S, Gorshkova IA, Usatyuk PV, He D, Pennathur A, Lambeth JD, Thannickal VJ, Natarajan V. Role of NOX4 and NOX2 in hyperoxia-induced reactive oxygen species generation and migration of human lung endothelial cells. *Antioxid Redox Signal* 2009;11:747-764.
PUBMED | CROSSREF

22. Kim J, Seo M, Kim SK, Bae YS. Flagellin-induced NADPH oxidase 4 activation is involved in atherosclerosis. *Sci Rep* 2016;6:25437.
PUBMED | CROSSREF

23. Moon JS, Nakahira K, Chung KP, DeNicola GM, Koo MJ, Pabón MA, Rooney KT, Yoon JH, Ryter SW, Stout-Delgado H, et al. NOX4-dependent fatty acid oxidation promotes NLRP3 inflammasome activation in macrophages. *Nat Med* 2016;22:1002-1012.
PUBMED | CROSSREF

24. Kim JH, Lee J, Bae SJ, Kim Y, Park BJ, Choi JW, Kwon J, Cha GH, Yoo HJ, Jo EK, et al. NADPH oxidase 4 is required for the generation of macrophage migration inhibitory factor and host defense against *Toxoplasma gondii* infection. *Sci Rep* 2017;7:6361.
PUBMED | CROSSREF

25. Fu P, Mohan V, Mansoor S, Tiruppathi C, Sadikot RT, Natarajan V. Role of nicotinamide adenine dinucleotide phosphate-reduced oxidase proteins in *Pseudomonas aeruginosa*-induced lung inflammation and permeability. *Am J Respir Cell Mol Biol* 2013;48:477-488.
PUBMED | CROSSREF

26. Neupane AS, Willson M, Chojnacki AK, Vargas E Silva Castanheira F, Morehouse C, Carestia A, Keller AE, Peiseler M, DiGiandomenico A, Kelly MM, et al. Patrolling alveolar macrophages conceal bacteria from the immune system to maintain homeostasis. *Cell* 2020;183:110-125.e11.
PUBMED | CROSSREF

27. McDonald KR, Hernandez-Nichols AL, Barnes JW, Patel RP. Hydrogen peroxide regulates endothelial surface N-glycoforms to control inflammatory monocyte rolling and adhesion. *Redox Biol* 2020;34:101498.
PUBMED | CROSSREF

28. Walpola PL, Gotlieb AI, Cybulsky MI, Langille BL. Expression of ICAM-1 and VCAM-1 and monocyte adherence in arteries exposed to altered shear stress. *Arterioscler Thromb Vasc Biol* 1995;15:2-10.
PUBMED | CROSSREF

29. Usui T, Ishida S, Yamashiro K, Kaji Y, Poulaki V, Moore J, Moore T, Amano S, Horikawa Y, Dartt D, et al. VEGF164(165) as the pathological isoform: differential leukocyte and endothelial responses through VEGFR1 and VEGFR2. *Invest Ophthalmol Vis Sci* 2004;45:368-374.
PUBMED | CROSSREF

30. Kim I, Moon SO, Kim SH, Kim HJ, Koh YS, Koh GY. Vascular endothelial growth factor expression of intercellular adhesion molecule 1 (ICAM-1), vascular cell adhesion molecule 1 (VCAM-1), and E-selectin through nuclear factor-kappa B activation in endothelial cells. *J Biol Chem* 2001;276:7614-7620.
PUBMED | CROSSREF

31. Radisavljevic Z, Avraham H, Avraham S. Vascular endothelial growth factor up-regulates ICAM-1 expression via the phosphatidylinositol 3 OH-kinase/AKT/Nitric oxide pathway and modulates migration of brain microvascular endothelial cells. *J Biol Chem* 2000;275:20770-20774.
PUBMED | CROSSREF

32. Kim YM, Kim SJ, Tatsunami R, Yamamura H, Fukai T, Ushio-Fukai M. ROS-induced ROS release orchestrated by NOX4, NOX2, and mitochondria in VEGF signaling and angiogenesis. *Am J Physiol Cell Physiol* 2017;312:C749-C764.
PUBMED | CROSSREF

33. Miyano K, Okamoto S, Yamauchi A, Kawai C, Kajikawa M, Kiyohara T, Tamura M, Taura M, Kuribayashi F. The NADPH oxidase NOX4 promotes the directed migration of endothelial cells by stabilizing vascular endothelial growth factor receptor 2 protein. *J Biol Chem* 2020;295:11877-11890.
PUBMED | CROSSREF

34. Steiner DJ, Furuya Y, Metzger DW. Detrimental influence of alveolar macrophages on protective humoral immunity during francisella tularensis schus4 pulmonary infection. *Infect Immun* 2018;86:e00787-17.
PUBMED | CROSSREF

35. Van Buul JD, Fernandez-Borja M, Anthony EC, Hordijk PL. Expression and localization of NOX2 and NOX4 in primary human endothelial cells. *Antioxid Redox Signal* 2005;7:308-317.
PUBMED | CROSSREF

36. Ago T, Kitazono T, Ooboshi H, Iyama T, Han YH, Takada J, Wakisaka M, Ibayashi S, Utsumi H, Iida M. NOX4 as the major catalytic component of an endothelial NAD(P)H oxidase. *Circulation* 2004;109:227-233.
PUBMED | CROSSREF

37. Carnesecchi S, Deffert C, Donati Y, Basset O, Hinz B, Preynat-Seauve O, Guichard C, Arbiser JL, Banfi B, Pache JC, et al. A key role for NOX4 in epithelial cell death during development of lung fibrosis. *Antioxid Redox Signal* 2011;15:607-619.
PUBMED | CROSSREF

38. Kim HJ, Park YD, Moon UY, Kim JH, Jeon JH, Lee JG, Bae YS, Yoon JH. The role of NOX4 in oxidative stress-induced MUC5AC overexpression in human airway epithelial cells. *Am J Respir Cell Mol Biol* 2008;39:598-609.
PUBMED | CROSSREF

39. Lee CF, Ullevig S, Kim HS, Asmis R. Regulation of monocyte adhesion and migration by nox4. *PLoS One* 2013;8:e66964.
PUBMED | CROSSREF

40. Ullevig S, Zhao Q, Lee CF, Seok Kim H, Zamora D, Asmis R. NADPH oxidase 4 mediates monocyte priming and accelerated chemotaxis induced by metabolic stress. *Arterioscler Thromb Vasc Biol* 2012;32:415-426.
PUBMED | CROSSREF

41. Fu P, Ramchandran R, Sudhadevi T, Kumar PP, Krishnan Y, Liu Y, Zhao Y, Parinandi NL, Harijith A, Sadoshima J, et al. Nox4 mediates *Pseudomonas aeruginosa*-induced nuclear reactive oxygen species generation and chromatin remodeling in lung epithelium. *Antioxidants* 2021;10:477.
PUBMED | CROSSREF

42. Kevil CG, Patel RP, Bullard DC. Essential role of ICAM-1 in mediating monocyte adhesion to aortic endothelial cells. *Am J Physiol Cell Physiol* 2001;281:C1442-C1447.
PUBMED | CROSSREF

43. Yang L, Froio RM, Sciuto TE, Dvorak AM, Alon R, Luscinskas FW. ICAM-1 regulates neutrophil adhesion and transcellular migration of TNF-alpha-activated vascular endothelium under flow. *Blood* 2005;106:584-592.
PUBMED | CROSSREF

44. Sumagin R, Brazil JC, Nava P, Nishio H, Alam A, Luissint AC, Weber DA, Neish AS, Nusrat A, Parkos CA. Neutrophil interactions with epithelial-expressed ICAM-1 enhances intestinal mucosal wound healing. *Mucosal Immunol* 2016;9:1151-1162.
PUBMED | CROSSREF

45. Regal-McDonald K, Patel RP. Selective recruitment of monocyte subsets by endothelial n-glycans. *Am J Pathol* 2020;190:947-957.
PUBMED | CROSSREF

46. Scott DW, Dunn TS, Ballestas ME, Litovsky SH, Patel RP. Identification of a high-mannose ICAM-1 glycoform: effects of ICAM-1 hypoglycosylation on monocyte adhesion and outside in signaling. *Am J Physiol Cell Physiol* 2013;305:C228-C237.
PUBMED | CROSSREF

47. Mizgerd JP. Molecular mechanisms of neutrophil recruitment elicited by bacteria in the lungs. *Semin Immunol* 2002;14:123-132.
PUBMED | CROSSREF

48. Vieira SM, Lemos HP, Grespan R, Napimoga MH, Dal-Secco D, Freitas A, Cunha TM, Verri WA Jr, Souza-Junior DA, Jamur MC, et al. A crucial role for TNF-alpha in mediating neutrophil influx induced by endogenously generated or exogenous chemokines, KC/CXCL1 and LIX/CXCL5. *Br J Pharmacol* 2009;158:779-789.
PUBMED | CROSSREF

49. Zasłona Z, Wilhelm J, Cakarova L, Marsh LM, Seeger W, Lohmeyer J, von Wulffen W. Transcriptome profiling of primary murine monocytes, lung macrophages and lung dendritic cells reveals a distinct expression of genes involved in cell trafficking. *Respir Res* 2009;10:2.
PUBMED | CROSSREF

50. Schagat TL, Wofford JA, Wright JR. Surfactant protein A enhances alveolar macrophage phagocytosis of apoptotic neutrophils. *J Immunol* 2001;166:2727-2733.
PUBMED | CROSSREF

51. Wong CK, Smith CA, Sakamoto K, Kaminski N, Koff JL, Goldstein DR. Aging impairs alveolar macrophage phagocytosis and increases influenza-induced mortality in mice. *J Immunol* 2017;199:1060-1068.
PUBMED | CROSSREF

52. Serhan CN, Chiang N, Dalli J, Levy BD. Lipid mediators in the resolution of inflammation. *Cold Spring Harb Perspect Biol* 2014;7:a016311.
PUBMED | CROSSREF

53. Knapp S, Leemans JC, Florquin S, Branger J, Maris NA, Pater J, van Rooijen N, van der Poll T. Alveolar macrophages have a protective antiinflammatory role during murine pneumococcal pneumonia. *Am J Respir Crit Care Med* 2003;167:171-179.
PUBMED | CROSSREF

54. Hou F, Xiao K, Tang L, Xie L. Diversity of macrophages in lung homeostasis and diseases. *Front Immunol* 2021;12:753940.
PUBMED | CROSSREF

55. Puttur F, Gregory LG, Lloyd CM. Airway macrophages as the guardians of tissue repair in the lung. *Immunol Cell Biol* 2019;97:246-257.
PUBMED | CROSSREF

56. Aegerter H, Kulikauskaite J, Crotta S, Patel H, Kelly G, Hessel EM, Mack M, Beinke S, Wack A. Influenza-induced monocyte-derived alveolar macrophages confer prolonged antibacterial protection. *Nat Immunol* 2020;21:145-157.
PUBMED | CROSSREF